ISSN 0915-633X

NATIONAL INSTITUTE FOR FUSION SCIENCE

Characterization of Local Turbulence in Magnetic Confinement Devices

M. Rajković, M. Škorić, K. Sølna, G. Antar

(Received - June 21, 2007)

NIFS-877 July 2007

RESEARCH REPORT
NIFS Series

TOKI, JAPAN

This report was prepared as a preprint of work performed as a collaboration research of the National Institute for Fusion Science (NIFS) of Japan. The views presented here are solely those of the authors. This document is intended for information only and may be published in a journal after some rearrangement of its contents in the future.

Inquiries about copyright should be addressed to the Research Information Office, National Institute for Fusion Science, Oroshi-cho, Toki-shi, Gifu-ken 509-5292 Japan.

E-mail: bunken@nifs.ac.jp

<Notice about photocopying>

In order to photocopy any work from this publication, you or your organization must obtain permission from the following organizaion which has been delegated for copyright for clearance by the copyright owner of this publication.

Except in the USA

Japan Academic Association for Copyright Clearance (JAACC)
6-41 Akasaka 9-chome, Minato-ku, Tokyo 107-0052 Japan
Phone: 81-3-3475-5618 FAX: 81-3-3475-5619 E-mail: jaacc@mtd.biglobe.ne.jp

In the USA

Copyright Clearance Center, Inc.
222 Rosewood Drive, Danvers, MA 01923 USA
Phone: 1-978-750-8400 FAX: 1-978-646-8600

Characterization of Local Turbulence in Magnetic Confinement Devices

Milan Rajković
Institute of Nuclear Sciences Vinča, Belgrade, Serbia,

Miloš Škorić
National Institute for Fusion Science, Toki, Gifu, Japan,

Knut Sølna,
Department of Mathematics, University of California Irvine, U.S.A

Ghassan Antar,
Fusion Energy Research Program,

University of California San Diego, U. S. A.

July 11, 2007

Abstract

A multifractal analysis based on evaluation and interpretation of Large Deviation spectra is applied to plasma edge turbulence data from different devices (MAST and Tore Supra). It is demonstrated that in spite of some universal features there are unique characteristics for each device as well as for diferent confinement regimes. In the second part of the exposition the issue of estimating the variable power law behavior of spectral densities is addressed. The analysis of this issue is performed using fractional Brownian motion (fBm) as the underlying stochastic model whose parameters are estimated locally in time by wavelet scale spectra. In such a manner information about the inertial range as well as variability of the fBm parameters is obtained giving more information important for understanding edge turbulence and intermittency.

1. Introduction

Plasma edge turbulence, known for a long time to be intermittent in the scrape-off layer [1] , is in focus of intense current research efforts aimed to understanding plasma confinement and dynamics of turbulent transport in magnetic fusion devices which represent important issues related to the control of confined plasma. Turbulence studies of the scrape-off layer (SOL) have revealed that intermittency in this region is caused by large-scale coherent structures with high radial velocity designated as blobs (or avaloids). A natural route for understanding turbulence and intermittency in the edge region of confinement devices and related transport properties is to search for universal properties and differences between dynamics of different systems and regimes. The first studies performed in this direction have concentrated on search for long-range dependence properties of plasma density fluctuations as well as on their eventual self-similar properties [2], [3]. Self-similar processes were attractive models to describe scalings of plasma fluctuations due to the fact that they are well documented and mathematically well-defined. In addition they are relatively simple and parsimonious and each of their properties are controlled by the one unique parameter, H, known as the Hurst parameter. It was soon realized that in spite of observed self-similarity for several confinement devices, over the mesoscale range of time scales , i.e. scales between 10 times the turbulence decorrelation time and plasma confinement time, different scaling laws exist in different time scale ranges. Hence, it became clear that self-similar processes are not adequate to model the extremely complex plasma turbulence fluctuations. Existence of long-range correlations, noticed in several magnetic confinement devices, suggested that scaling models with a single parameter are appropriate at large scales but at small scales, characteristic for intermittency, more parameters are needed. As a consequence, a need for multifractal analysis, an extension of monofractal analysis which is based on self-similarity concept, was recognized relatively recently. In spite of that, only few studies were devoted to the multifractal analysis of plasma fluctuations and more importantly a multifractal analysis tools used were inadequate to recognize subtle differences in various confinement devices and hence deviations from universal characteristics [4], [5].

Plasma turbulence studies, usually rely on results obtained for neutral fluid turbulence which may be beneficial from many aspects although care must be taken in recognizing differences and specific features of each. In particular, nonlinearites in plasma turbulence are more numerous having different spectral cascade directions in addition to the $E \times B$ nonlinearity, leading to more complex

fluctuating characteristics. One of the most important differences is that time and space measurements lead to different information on the structure of turbulence [6]. Driving mechanisms and damping characteristics are reflected in the temporal aspect of fluctuations while measurements at different spatial locations provide information on spatial structures for various scale lengths. For the case of neutral fluids, time records of turbulent velocity at a single spatial location obtained with the use of a hot-wire or laser Doppler anemometer, are usually interpreted via Taylor's frozen flow hypotheses, as one-dimensional spatial cuts through the flow. However, this approach that generates information about temporal measurements from spatial ones and vice versa, is not applicable in the case of plasma turbulence. Specifically, turbulence in the case of neutral fluids is generated at a certain spatial position and carried by the flow past the probe location so that recordings at different times at a fixed location are equivalent to simultaneous recordings at different spatial locations along the flow. However, in plasma turbulence due to specific nature of nonlinearities, turbulence is created and damped at the same spatial position where the measurements are taken so that spatial and temporal informations are interwoven. For the same reason the inertial range [7], may exist only locally in space or in time, and the extent of this range changes along the temporal scale as well as along space, for example along poloidal direction. One of the main results of the study presented here is to establish the existence of local (in time) inertial range and to estimate its scaling properties for various devices and confinement regimes. Proving the existence of local inertial range and evaluating its characteristics may be of great importance, among other things, in generating synthetic random media for simulation of wave propagation in turbulent plasma, relevant for Doppler reflectometry for example.

One of the first important issues to be agreed upon in the analysis of plasma turbulence, and in particular intermittency and its multifractal character, is the choice of relevant measure. In neutral fluid turbulence, in addition to velocity, enstrophy and energy dissipation represent quantities of particular interest although they cannot be constructed in their entirety from a single point velocity time-series. These quantities are usually replaced by the so-called surrogate fields which take the form of a single component of a many component fields. Intermittency is usually studied via energy dissipation rate whose complete expression is given by

$$\epsilon(\overrightarrow{r}) = \frac{\nu}{2} \sum_{i,j} \left(\partial_i v_j + \partial_j v_i\right)^2 , \tag{1}$$

where indices i and j represent coordinate axes. This expression evidently can-

not be constructed from recorded time-series as usually only the longitudinal and transverse components of velocity, v_x and v_y respectively, are measured. To overcome the difficulty, expression 1 is replaced by the so called surrogate dissipation

$$\epsilon_{surr}(x) = C\nu \left(\frac{\partial v_x}{\partial x} \right)^2, \tag{2}$$

where C is a constant, sometimes taken equal to 15 [8]. Using Taylor's frozen flow hypothesis which is naturally justified in neutral fluid turbulence, expression 2 becomes

$$\epsilon_{surr}(t) \sim \nu \left(\frac{\partial v_x}{\partial t} \right)^2. \tag{3}$$

An important measure quantifying intermittency is the so-called intermittency exponent. As proposed in [9], it may be extracted from the slope of the two-point correlation function of energy dissipation field. This procedure may be used to develop a criterion for constructing a measure, analogous to the surrogate dissipation, relevant for plasma turbulence and intermittency. In [10], it was demonstrated that normalized two-point correlation function $\langle \epsilon_{surr}(x + \Delta x)\epsilon_{surr}(x) \rangle \, / \, \langle \epsilon_{surr}(x) \rangle^2$ scales as $\sim \Delta x^{-\mu}$, where μ is the intermittency exponent. Studies in this reference and in [8], for the case of atmospheric turbulence, and studies in [11] and [12], for the gaseous helium jet, found $\mu \simeq 0.22$, independent of the Reynolds number.

In the exposition that follows we assume that ion saturation current fluctuations, the only measured quantity used in this exposition, are equivalent to density fluctuations as justified in detail in [13] . Based on the above description for the case of neutral fluid turbulence, we set as the goal to construct a measure analogous to surrogate dissipation whose scaling of two-point correlation function of L-mode fluctuations would yield an intermittency exponent as close to the value for neutral fluid turbulence, as possible. The reason for choosing L-mode fluctuations is supported by results presented further on in this study, which imply that L-mode intermittent fluctuations are very similar in their fractal and multifractal aspects to the neutral fluid intermittency. A search for appropriate measure, based on heuristic arguments, was described in [4], and proposed measures are

$$\epsilon_n = \frac{(n - \langle n \rangle)^2}{\left\langle (n - \langle n \rangle)^2 \right\rangle}, \tag{4}$$

and

$$\epsilon_{\delta n} = \frac{\left(\frac{dn}{dt} - \left\langle \frac{dn}{dt} \right\rangle \right)^2}{\left\langle \left(\frac{dn}{dt} - \left\langle \frac{dn}{dt} \right\rangle \right)^2 \right\rangle}. \tag{5}$$

A similar measure with dn^2/dt replacing dn/dt in 5 was employed in [13]. However our study based on the analysis of L-mode fluctuations in MAST, Tore Supra and PISCES devices, indicates that these two measures yield too high or too low values for the intermittency exponent. The following two measures

$$\epsilon = c \cdot \frac{\left(\left|n\frac{dn}{dt}\right| - \left\langle\left|n\frac{dn}{dt}\right|\right\rangle\right)^2}{\left\langle\left(\left|n\frac{dn}{dt}\right| - \left\langle\left|n\frac{dn}{dt}\right|\right\rangle\right)^2\right\rangle}, \tag{6}$$

and

$$\epsilon = c \cdot \frac{\left(\left(n\frac{dn}{dt}\right)^2 - \left\langle\left(n\frac{dn}{dt}\right)^2\right\rangle\right)^2}{\left\langle\left(\left(n\frac{dn}{dt}\right)^2 - \left\langle\left(n\frac{dn}{dt}\right)^2\right\rangle\right)^2\right\rangle}, \tag{7}$$

where c is a constant, which upon evaluation of the slope of two-point correlation function yield intermittency exponent $\mu \sim 0.3$, a value closer to the μ of neutral fluid intermittency than the values obtained from two-point correlation functions of measures 4 and 5. A comparative schematic representation of slopes of two-point correlation functions for three different measures is presented in Fig. 1. It should be emphasized that measures in expressions 6 and 7 are by no means expressions for dissipation but rather surrogate quantities whose multifractal and two-point correlation function properties give accurate information about burstiness property of the ion saturation current (i.e. plasma density). Namely, one kind of burstiness arises from dependencies over long time periods as reflected in the long-range correlation property and the second kind of burstiness arises from fluctuations in amplitude and therefore concerns small scale behavior. These two types of burstiness are well captured and quantified within the multifractal formalism by measures that we propose here, 6 and 7.

The rest of the paper is organized as follows. In Sec. II we present basic features of multifractal processes with special emphasis on large deviation spectra. In Sec. III we present multifractal characteristics of L-mode and dithering H-mode of the MAST device, and the L-mode of the Tore Supra device. This analysis is based on the large deviation spectra which reveal features unobtainable using the traditional Legendre or Hausdorff multifractal spectra. In Sec. IV local features of turbulence are modelled using fractional Brownian motion and wavelet techniques and in Sec. V we present results pertaining to the two devices considered. Finally, in Sec. VI we present our conclusions related to the universal and idiosyncratic aspects of obtained results.

2. Multifractal Measures and Properties

Multifractal measures can be built by iterating a simple procedure called a *multiplicative cascade* whose various forms are used to model the energy dissipation field of fully developed turbulence, physically motivated by Richardson cascade model of energy transfer from large to small scales by random breakup of eddies. The simplest example of such cascades is the binomial measure on $I = [0, 1]$ (e.g. [14]). Consider the uniform probability measure μ_0 on I, and split the unit interval I into two subintervals $I_0 = [0, 1/2]$ and $I_1 = [1/2, 1]$. In the process mass m_0 is spread uniformly over I_0 and m_1 is spread over I_1 so that $m_1 = 1 - m_0$ and it is obvious that the density of measure μ_1 is a step function. With the two subintervals the procedure is repeated in the same manner so that at the second stage the measures are $\mu_2[I_{00}] = m_0 m_0$, $\mu_2[I_{01}] = m_0 m_1$, $\mu_2[I_{10}] = m_1 m_0$ and $\mu_2[I_{11}] = m_1 m_1$. At stage n, the conserved mass equal to 1 is distributed among the 2^n dyadic intervals $I_{\varepsilon_1 \ldots \varepsilon_n}$ according to all possible products $\mu(I_{\varepsilon_1 \ldots \varepsilon_n}) = m_{\varepsilon_1} \ldots m_{\varepsilon_n}$, where m_{ε_i} are denoted as multipliers. Iteration of this procedure generates an infinite sequence of measures $\{\mu_n\}$ that weakly converge to the binomial measure μ. The construction creates large and increasing heterogeneity in the allocation of mass leading to the multifractal properties. The binomial, like many multifractals, is continuous but singular probability measure that has no density and no point mass. An extension of such a procedure, more relevant for turbulence phenomena, randomizes the allocation of mass between subintervals and another procedure, also of relevance for turbulence research, may also be employed with arbitrary distribution of multipliers (with mass being conserved either at each stage of the process or preserved only on the average) yielding multiplicative measures characteristic of multifractals. The relevance of such cascade processes in turbulence is discussed in, for example, [7], [15].

Multifractality of measures is easily extended to functions so that a stochastic process $X(t)$ is called multifractal if it has stationary increments and satisfies

$$E\left(|X(t)|^q\right) = c(q) t^{\tau(q)+1},$$

for all t and q belonging to intervals on the real line, and where $\tau(q)$ and $c(q)$ are functions with domain on the real line. The function $\tau(q)$ is called the scaling function of the multifractal process. It may be easily proved that $\tau(q)$ is concave, and for self-similar processes, controlled by one exponent H, it assumes a simple form

$$\tau(q) = Hq - 1,$$

with H known as the Hurst exponent. The corresponding process is called monofractal. For multifractal processes $\tau(q)$ is nonlinear. The Legendre transform of the scaling function $\tau(q)$ is called the Legendre multifractal spectrum:

$$f(\alpha) = \underset{q}{Inf}\ [\alpha q - \tau(q)].$$

In the above expression α is the local Hölder exponent, whose meaning may be defined in the following way. Let $\epsilon(t)$ denote the measure given either by expression 6 or expression 7 at time $t \in [0, T]$ so that the infinitesimal variation of measure ϵ around time t is heuristically of the form

$$|\ln \epsilon(t + dt) - \ln \epsilon(t)| \sim C_t (dt)^{\alpha(t)},$$

where $\alpha(t)$ is called the local Hölder exponent, while C_t is the prefactor at t. From this definition it is apparent that $\alpha(t)$, also known as local scale at t, quantifies the scaling properties of the process at a given point in time so that lower values correspond to more abrupt variations. Multifractal processes contain a continuum of local scales and such a continuum is reflected in the smooth Legendre spectrum $f(\alpha)$. Hence the multifractal spectrum represents a convenient representation for the distribution of Hölder exponents. The shape of the spectrum is very sensitive to the distribution of multipliers so that it may give important information about multiplicative processes.

2.1. Large Deviation Spectrum

As mentioned earlier, the mulitfractal spectrum evaluated by performing the Legendre transform of the scaling function is a smooth function of local Hölder exponents. However sometimes more information may be obtained from the multifractal spectrum derived by applying the Large Deviation Theory. Noticing that the Hölder exponent may be defined as the lim inf of the ratio

$$\ln |\epsilon(t + \Delta t) - \epsilon(t)| \,/\, \ln(\Delta t) \quad \text{as} \quad \Delta t \to 0,$$

it is suggestive to estimate the distribution of local Hölder exponents at a random instant. For that reason partition $[0, T]$ into 2^k subintervals $[t_i, t_i + \Delta t]$, where length $\Delta t = 2^{-k} T$, and calculate for each subinterval the *coarse Hölder exponent*

$$\alpha_k(t_i) \equiv \ln |\epsilon(t_i + \Delta t) - \epsilon(t_i)| \,/\, \ln(\Delta t),$$

so that a set $\{\alpha_k(t_i)\}$ of 2^k observations is formed. The range of Hölder exponents is then divided into small intervals $\Delta\alpha$, and let $N_k(\alpha)$ be the number of coarse exponents contained in $(\alpha,\ \alpha + \Delta\alpha]$. Proceeding further, one could calculate a histogram with relative frequencies $N_k(\alpha)/2^k$, which for $k \to \infty$ converge to the probability that a random time moment t has Hölder exponent α. However since multifractals typically have a dominant exponent α_0 implying that $\alpha(t) = \alpha_0$ at almost every instant, the obtained histogram would degenerate into a delta function, failing to give relevant information on a multifractal process. Instead, the multifractal spectrum in the context of the Large Deviation Principle [14], denoted as Large Deviation Spectrum is defined as

$$f_{LDS}(\alpha) := \lim_{k\to\infty} \sup \frac{\ln N_k(\alpha)}{\ln 2^k},$$

so that it represents the renormalized probability distribution of local Hölder exponents. Indeed, $N_k(\alpha)/2^k$ defines a probability distribution on $\{\alpha_i : i = 0, ..., 2^k - 1\}$. Referring to the Law of Large Numbers and the arguments given earlier, it is expected that this distribution is concentrated more and more about the most expected value as k increases so that $f_{LDS}(\alpha)$ measures how fast the probability $N_k(\alpha)/2^k$ to observe an atypical value of α decreases, i.e., $N_k(\alpha)/2^k \simeq 2^{f(\alpha)-1}$. As far as the Large Deviation Spectrum of multiplicative measures is concerned, it directly depends on the asymptotic distribution of α_k which in turn depends on the distribution of multipliers. Actually, most of the mass of the multiplicative cascade concentrates on intervals with Hölder exponents bounded away from the most probable value α_0, so that the Large Deviation Spectrum gives important information on these "rare events". A usually determined Legendre multifractal spectrum is concave by definition and represents the convex hull of the Large Deviation Spectrum.

3. Large Deviation Spectra of plasma turbulence intermittency

The goal of this section is to present a comparative study of Large Deviation Spectra of the boundary plasma turbulence intermittency in the scrape-off layer (SOL). The ion saturation current fluctuations of reciprocating Langmuir probe installed at the edge of magnetic confinement devices are used to this purpose. Recent experimental studies have suggested that intermittency in the SOL of magnetic confinement devices is caused by nonlocally coherent structures denoted

as blobs or avaloids [16] , which essentially are large-scale structures with high radial velocity, ejected radially towards the wall and encountered intermittently in SOL. These structures lead to a direct loss of matter and energy and hence have a high impact on confinement in contrast to the second type of coherent structures which may exist in fusion devices, which represent locally organized fluctuations and which, due to their non radial propagation, contribute less to the loss of confinement. We study intermittency properties of two different devices, the MAST spherical tokamak (L- and dithering H-mode) and the Tore Supra tokamak with limiter configuration (L-mode).

3.1. MAST spectra

The datasets analyzed here consist of measurements of the ion saturation current (I_{SAT}) performed by the moveable Langmuir probe located at the outboard midplane on MAST device [17], [18]. Sampling rate was 1 MHz and during the discharge the distance from the plasma edge to the probe changed slowly. For this reason, time-periods during which the distance was approximately constant so that plasma current and confinement modes were constant, were chosen for the analysis. The analysis of two confinement regimes, L-mode and dithering H-mode is presented here. Discharge 6861 is high density L-mode plasma and 9031 represents a dithering H-mode with heating power close to the threshold for L-H transition with intermittent high frequency edge localized modes (ELMs). Time-series of L-mode and dithering H-mode signals are presented in Figs. 2 and 3.respectively. Other relevant discharge parameters are presented in Table 1.

Table 1. Discharge parameters for MAST data

	Plasma current (kA)	Normalized electron density n_e/n_G	Probe distance from plasma edge (cm)	Duration of signal (ms)
6861 L	665	0.69	4.4±0.1	40
9031 L/H	535	0.42	5.7±1.0	88

The large deviation spectra for 6861 L-mode and 9031 dithering H-mode are presented in Figs. 4 and 5 respectively on five different scales, namely for $\Delta t = 2^3, ..., 2^7$. The most striking feature of these spectra is their departure from a pure bell-shape and concavity and is a good example where Large Deviation Spectra provide more information than Legendre spectra, which are strictly con-

cave although they may be asymmetrical. One possible explanation for such a behavior is that there are more multiplicative laws underlying the cascade processes so that there is a lumping of measures whose supports are disjoint [19]. In Fig. 6 the lumping of two measures with disjoint supports is presented generating a spectrum consisting of maximal parts of individual spectra, and illustrating the mechanism of concavity deformation in the LD spectrum. Also, superposition of more measures may lead to the departure from concavity in the LD plasma spectra, to produce effects similar to the ones observed in Figs. 4 and 5 [19]. In such a case the construction of two or more measures is identical from the geometrical point of view, however the difference stems from the choice of multipliers. In either case there is a sort of phase transition so that the process contributing mostly to the singularities corresponding to a specific Hölder exponent α, changes from one measure to another. It is evident that the L-mode has more complex multifractal structure in the sense that more measures, three in this case, are lumped than in the case of dithering H-mode, and consequently the cascade mechanism and energy transfer is more complex. The right-hand slope of the spectra, both in the case of L- an the L/H- mode, is larger than the left-hand slope, indicating rich variety of strong singularities and their gradual probability of occurrence.

When α is less than the most probable value of Hölder exponent α_0, it corresponds to divergent singularities since $\epsilon(t) \to \infty$ as $t \to 0$, while when $\alpha > \alpha_0$ it reflects regular (bounded) singularities since $\epsilon(t) \to 0$ as $t \to 0$. The fact that both spectra are not symmetric again emphasizes the fact that the processes involved are not purely multiplicative. This implies that the energy across scales is not transported through the generation of vortices and hence that it is not conserved at each step of the process, although it may be conserved on the average. This is closely related to random multiplicative cascades mentioned earlier with mass being conserved not at each stage of the process but on the average. The width of the spectrum, defined as the $|\alpha_{\max} - \alpha_{\min}|$, is larger in the case of L-mode, due to the stronger intermittency effects. Moreover, more irregular instants (degenerate singularities) of fluctuations are present in the L-mode than in the dithering H-mode since in the former case the width $|\alpha_{\min} - \alpha_0|$ is larger than in the later case. Note also the location of the most probable Hölder exponent α_0, as $\alpha_0 \sim 0.6$ for the L-mode and slightly larger $\alpha_0 \sim 0.7$ for the dithering H-mode. As mentioned earlier the shape of the spectra is determined by the distribution of multipliers of the multiplicative process and this issue will be addressed in detail elsewhere [20].

As a final remark we mention that measures in expressions 6 and 7 proposed here as multifractal dissipation measures, for different dyadic intervals

$\Delta t = 2^k (k = 1, 2, ..)$ produce Large Deviation spectra whose most probable Hölder exponents coincide, which is not the case for other measures, such as 4 and variations of it. Hence, evaluation of Large Deviation spectra, in addition to two-point correlation functions, supports the choice for these measures.

3.1.1. Tore Supra spectra

The data were collected on the Tore Supra tokamak, a fusion device with a major and minor radii equal to $R = 2.32$ m and $a = 0.76$ m, respectively. The reciprocating Langmuir probe, installed on the top of the Tore Supra tokamak, contains two sets of three composite carbon tips with 6 mm diameter toroidally separated by a distance of 20 mm. The probe is immersed into the plasma of SOL at a predetermined position and comes back in ~ 150 ms. Several plunges are performed during each discharge and 8000 data points were recorded at a frequency of 1MHz. Detailed description of probes and data acquisition procedure is described in [13]. Four different signals, each of 8 ms duration are analyzed here, and a sample of the time series is shown in Figs. 7 and 8.

Large Deviation Spectra of the four signals are presented in Figs. 9-12. As in the case of MAST turbulence data, rather than looking at the exact values of the LDS spectra, considerable amount of information may be obtained by inspecting the shape of the spectra. The most striking feature in the spectra is nonexistence or very mild lumping of measures with no superposition of measures. This is in large contrast to the MAST intermittency where lumping of measures is the most noticeable feature in the shape of the spectra. More interestingly, the mild lumping occurs for measures corresponding to regular singularities while strong lumping in MAST intermittency corresponds to divergent singularities. The overall shape of the spectra and the arguments given above lead to the conclusion that statistical distribution of multiplicative cascade multipliers is completely different in the case of Tore Supra edge turbulence as compared to the MAST case implying different energy transport processes and different nonmultiplicative mechanisms which accompany energy transfer across scales in two devices. Without getting into details of calculations, we mention here that distribution of multipliers of the multiplicative cascade in the MAST turbulence is exponential while for the Tore Supra device it is log-normal [20]. Another important feature of the Tore Supra spectra is their smaller width $\alpha_{\max} - \alpha_{\min}$. However, more striking is the smaller range of divergent singularities $|\alpha_{\min} - \alpha_0|$, corresponding to smaller number of rare fluctuations. Hence, not only is the edge intermittency weaker in Tore Supra

fluctuations, it is less abundant in rare events.

Based on the above comparative analysis, in spite of the universal multifractal character of fluctuations, there are significant differences with important implications and care must be taken when generalizing certain properties of fluctuations and when turning to specific features characteristic of a distinct device. Proceeding further with the aim of better understanding edge turbulence properties in fusion devices we undertake the analysis, presented in the next two sections, to provide time localized information about the essential frequency content of the fluctuations and about the existence of inertial range.

4. Estimation of local turbulence properties

Turbulent fluctuations, although highly nonstationary, usually exhibit approximate stationarity in the appropriately chosen segments over which spectral densities exhibit approximate power law scaling. Estimation of the power law behavior of spectral densities from measured plasma edge fluctuations is based upon appropriate segmentation of the data and the choice of frequencies over which the search for power law behavior is performed. The analysis presented here is based on the method and software presented in [21] The motivation for a such a procedure is twofold. The first is to estimate the local temporal variations in the correlation properties of the fluctuations and to evaluate the variation of the absolute level of these correlations. The second is the propagation of microwaves in plasma for the purpose of Doppler reflectometry used for estimating plasma rotation profiles and turbulence properties. The plasma medium may be modelled based on the fractional Brownian motion (fBm) and we use fBm as a model for local turbulence.

Fractional Brownian motion represents the most simple local power law process which is nonstationary but with stationary increments. The variance of the stationary increments is quantified by the structure function given by

$$E\left\{(B_H(t+\Delta t)-B_H(t))^2\right\}=\sigma^2\left|\Delta t\right|^{2H}, \quad H\in[0,1]. \tag{8}$$

In the above expression the Hurst exponent H determines the correlation distance for the increments of the process and the quantity σ^2 quantifies the absolute level of correlations. Ordinary Brownian motion is characterized by a unique exponent $H = 1/2$, so that regarding its multifractal properties $B_H(t)$ has a local Hölder exponent $\alpha(t) = H$, i.e. it is a monofractal process. Fractional Brownian motion is self-similar since $B_H(t) = a^H B_H(t/a)$, were the equal sign implies equality in distribution. Increasing the exponent beyond this value, i.e.

$H > 1/2$ corresponds to positive correlations (persistence) and long memory, while the case of $H < 1/2$ corresponds to negative correlations (antipersistence). On a set of Lebesgue measure 1, the multifractal process with $H > 1/2$ is more regular than a Brownian motion. Since we are dealing with intermittent phenomena which exhibit multifractal properties, the power law parameters of the local power-law model, σ and H are functions of time and these variations are modelled as a secondary stochastic process. The other important feature of the fBm application in the context of edge turbulence data is that the model is applied only over a subset of scales known as the inertial range. Usually multifractal data, besides variations in σ and H, show variations in the inertial range itself. As explained in the Introduction, turbulence in plasma is created and damped at the same spatial location so the existence of the inertial range in plasma turbulence needs conclusive tests which we set as one of the goals of this study. Wavelet scale spectra are used for this purpose because they provide time-scale decomposition that is compliant with power law processes, independent of their stationarity.

4.1. Scale spectrum

Wavelet scale spectra are used for the purpose of fitting the estimated spectrum to a power law. Scale spectra are more flexible and adjustable to self-similar processes as verified in numerous studies, e.g.[22]. Haar wavelets with narrow support are a good choice for the analysis of turbulence due to their simplicity and versatility however other bases would be also suitable. Let

$$n = (a_0(1),\ a_0(2),\ \ldots\ a_0(2^M),$$

denote the plasma density data, i.e. ion saturation current fluctuations. Wavelet coefficients corresponding to the signal are then calculated and scale spectrum of n, relative to the Haar wavelet basis, is the sequence S_j defined by

$$S_j = \frac{1}{2^{M-j}} \sum\nolimits_{i=1}^{2^{M-j}} \left(d_j(i)\right)^2, \qquad j = 1, 2, ..., M,$$

where d_j are detail coefficients and j denotes the scale. The scale spectral point S_j is the mean square of the detail coefficients at scale j, so that the spectrum can be interpreted as representing energy of the signal at different scales. The main goal is now to test whether the edge turbulence data can be modelled in a satisfactory manner by a power law model over a subrange of scales. For the process modeled by the structure function given by expression 8 the scale spectrum S_j is linear in

the log log plot, assuming that the record is long enough. Actually, over a suitable range of scales the mean of the log scale spectrum over a long enough segment is given by expression

$$E(\log(S_j)) \approx c - p \log K_j,$$

where $p = -(2h+1), c = c(H, \sigma)$ is a known function and K_j is a spatial frequency [21]. Hence, local Hurst exponents may be calculated readily from the slope of the log scale spectrum. Of particular interest is the value of $H = 1/3$ which corresponds to the Kolmogorov's scaling. Other important issues, relevant for interpretation of results, such as the choice of segmentation and filtering to smooth out the effects of segmentation, are described in detail in [21]. Particularly sensitive is the former issue as the segmentation should be not too much larger than the interval of stationarity. The obtained results should be independent of segmentation which implies that changing the length of segments should not change the variability of the estimated parameters. Summarizing the procedure, an estimation of fBm is generalized to a procedure for determination of a local power law process. For processes under study, the power law (the exponent or slope) and the multiplicative constant (log intercept of the scale spectrum) are not constants. Instead, they both vary slowly and the estimation of the power law parameters and the multiplicative constant are performed by segmenting the data and then removing segmentation effects by a filtering procedure. An estimation procedure requires estimation of time dependent inertial ranges whose existence and extent also changes with time.

4.2. Local features of MAST and Tore Supra edge turbulence

Local turbulence modelling using fractional Brownian motion and wavelet basis scaling properties show that indeed inertial range in temporal domain exists and that it is possible to gain important information about edge turbulence properties using this approach. In particular, the scale spectra of MAST data reveal a similar scaling range for both the L-mode and dithering H_mode confinement. The variability of the inertial range itself in the dithering H-mode case is enhanced by the switching process from low to high confinement, so that it is practically the same as in the L-mode case. In Fig. 13 an inertial range for the case of L-mode 6861of the MAST device is presented obtained after careful segmentation and check for stationarity of the data. In Fig. 14 an inertial range for the L-mode (L1 signal) of the Tore Supra device is presented and a quick comparison with the L-mode MAST case reveals a larger extent of the scaling range. This is expected

based on the more regular and more symmetric Large Deviation spectra, implying less strong intermittency in the Tore Supra edge turbulence data. Figs. 15 and 16 present local temporal variations of the Hurst exponent and the variance of the fBm model 8. Both parameters show random fluctuations and in the case of L-mode turbulence data, local Hurst exponent fluctuates close to the Kolmogorov's value of 1/3, so that from that aspect of multifractality L-mode plasma turbulence is similar to the neutral fluid turbulence. In the case of dithering H-mode, Fig. 16, the average Hurst exponent value is lower than in the L-mode case however it exhibits distinct random variability from a minimum value of $H = 0.1$. Both cases are typical of multifractal processes which show fast, random fluctuations of the regularity parameter H.

Characteristics of local turbulence of the Tore Supra device are presented in Figs. 17 and 18, where cases (plunges) L1 and L4 are illustrated. Data L2 and L3 are not presented since they are very similar to the L1 case. The striking feature on both diagrams is slow, almost deterministic variation of the local Hurst exponent and the variance. For L4 data, variability is somewhat larger however it is almost periodic so that it reflects the deterministic like character of the L1 case. We may conclude that local processes on Figs. 17 and 18 display enough regularity which are not characteristic of the true multifractals. Actually, this particular sets of Tore Supra edge turbulence data are *multifractional*, rather then multifractal. This is the term used for processes which are not multifractal in the true sense since they may exhibit local irregularity as reflected in the H value that is "deterministic", meaning that it is almost the same or predictable for all realizations, whereas it is random for truly stochastic process. Moreover, H varies smoothly or very slowly while this is not the case in a true multifractal process. Some of these features may have been anticipated based on the shape of Large Deviation spectra however analysis local in time or in space provides necessary conclusiveness.

5. Conclusion

Multifractal tools have been employed in order to test the universality of the edge turbulence properties in various magnetic confinement devices. It was shown that Large Deviation spectra represent powerful tools enabling advanced insight into the multifractal processes and provide information that is sensitive to the data and hence to the confinement device in which the date were generated. Complemented by an analysis of local turbulence based on the fractional Brownian

motion and wavelet scaling properties it was shown that turbulence properties are different in the MAST device and the Tore Supra tokamak, suggesting that new studies involving different devices and possibly extensions of existing methods for the analysis should be undertaken. Shapes of Large Deviation Spectra clearly suggest different energy transport mechanisms in the two devices while local analysis reveals a multifractional character of the processes in the Tore Supra device in contrast to the genuine multifractal processes in the MAST device. In the light of results presented here the call for a careful interpretation of the universal characteristics of edge turbulence data is evident. In addition, differences over local temporal records of turbulence data for various devices show how important local modelling based on the fractional Brownian motion and wavelet scale spectra is for constructing accurate synthetic random medium for simulation of wave propagation in turbulent plasma.

Acknowledgement 1. *One of the authors, M.R., expresses gratitude for NIFS hospitality and support under the NINS-NIFS International Base Research Network funding and for continuing assistance to S. Ishiguro, A. Ito and H. Okumura. Stimulating discussions with R. Dendy, T. Watanabe and B. Dudson are greatfully acknowledged.*

References

[1] G. Antar, G. Counsell, Y. Yu, B. Lombard and P. Devynck, Phys. Plasmas 10 (2003) 419-428.

[2] G. Wang, G, Antar and P. Devynck, Phys. Plasmas 7 (2000) 1181.

[3] B. A. Carreras et al., Phys. Plasmas 10 (1998) 3632.

[4] B. Carreras, V.E. Lynch, D.E. Newman, R. Balbin, J. Bleuel, M.A. Pedrosa, M. Endler, B. van Milligen, E. Sánchez and C. Hidalgo, Physics of Plasmas, 7 (2000) 3278-3287.

[5] V. P. Budaev, S. Takamura, N. Ohno and S. Masuzaki, Nuclear Fusion 46 (2006) S181-S191.

[6] B. A. Carreras, E. R. Balbin, J. Bleuel, et al., Phys. Rev. Lett. (2000).

[7] U. Frisch, *Turbulence, the Legacy of A. N. Kolmogorov,* Cambridge University Press, Cambridge, 1995.

[8] J. Cleve, M. Greiner and K. R. Sreenivasan, Europhysics Lett., 61 (2003) 756-761.

[9] A. S. Monin and A. M. Yaglom, *Statistical Fluid Mechanics* vol. 2, MIT Press, Cambridge MA, 1971.

[10] J. Cleve, M. Greiner, B. R. Person and K. R. Sreenivasan, Phys. Rev. E 69 (2004) 066316.

[11] O. Channal, B. Chabaud, B. Castaing and B. Hébral, Eur. Phys. J. B 17 (2000) 309.

[12] J. Delour, J. F. Muzy and A. Arneodo, Eur. Phys. J B 23 (2001) 2443-248.

[13] G. Y. Antar, P. Devynck, X. Garbet and S. C. Luckhardt, Physics of Plasmas, 8 (2001) 1612.

[14] R. H. Riedi, J. Math. Anal. Appl. 189 (1995) 462-490.

[15] C. Menevau and K. R. Sreenivasan, J. Fluid Mech. 224 (1991) 429.

[16] G. Y. Antar, Phys. Rev. Lett. 87 (2001) 065001.

[17] G. F. Counsell at al., Nucl. Fusion 45 (2005) S157-S167.

[18] B. D. Dudson, R. O. Dendy, A. Kirk, H. Meyer and G. F. Councel, Plasma Phys. Control Fusion 47 (2005) 885-901.

[19] R. H. Riedi and J. L. Vehel, Technical report 3129, INRIA Rocquencourt, France, February 1997; available at www.dsp.rice.edu.

[20] M. Rajković, M. Škorić and R. Dendy (in preparation).

[21] K. SØlna and G. Papnicolaou, in *Long-range Dependence: Theory and Applications*, Editors P. Doukhan, G. Oppenmeim and M. S. Taqqu, 2002.

[22] P. Abry, P. Flandrin, M. S. Taqqu and D. Weitch, Chapter 2 in *Self Similar Network Traffic and Performance Evaluation*, Editors K. Park and W. Willinger, Wiley, 2000..

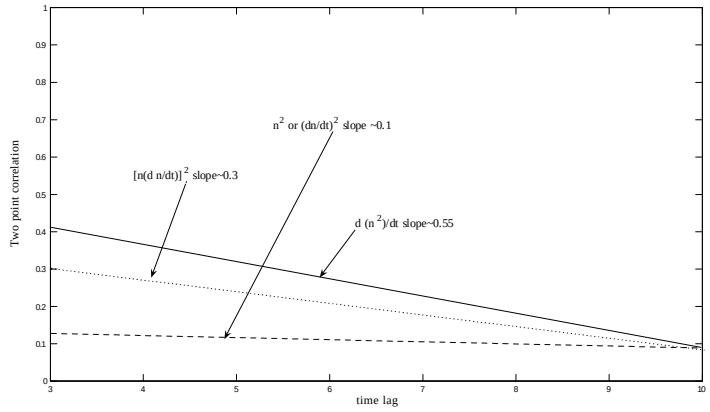

Figure 1: Schematic representation of two-point correlation function slopes corresponding to different multifractal dissipation measures. The optimal measure yields slope ~ 0.3.

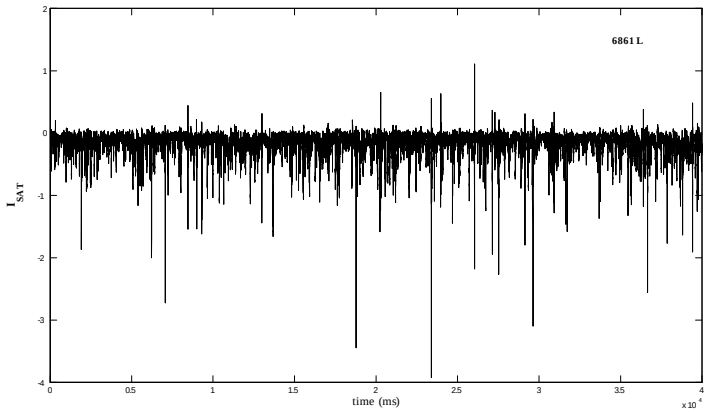

Figure 2: Saturation current fluctuations as a function of time for the low confinement regime 6861 of the MAST device.

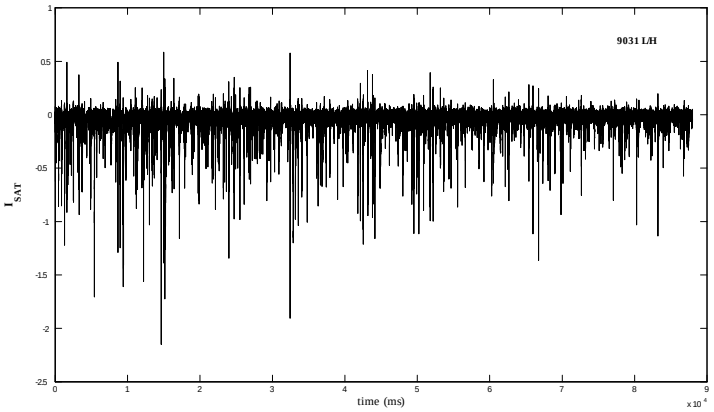

Figure 3: Saturation current fluctuations as a function of time for the dithering H mode confinement regime of the MAST device.

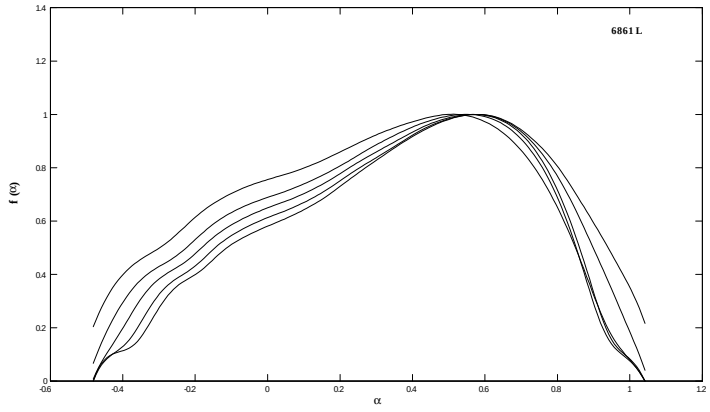

Figure 4: Large Deviation Spectrum for the L-mode signal 6861 of the MAST device for five different scales: $\Delta t = 2^3, ..., 2^7$. Lumping of measures is evident for singularities smaller than the most probable Hölder exponent.

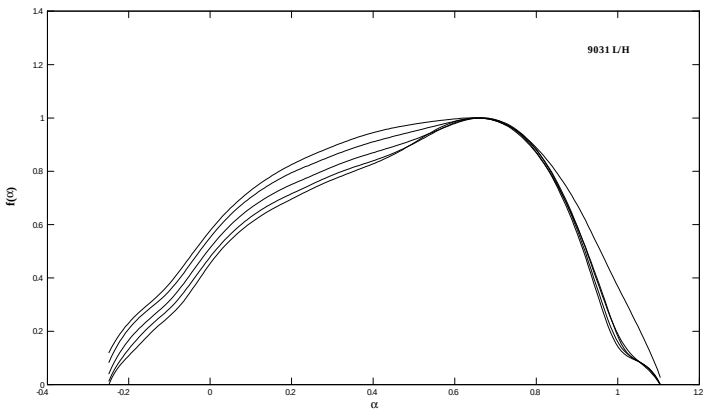

Figure 5: Large Deviation Spectrum for the dithering H-mode signal 9031 of the MAST device for $\Delta t = 2^3, ..., 2^7$.

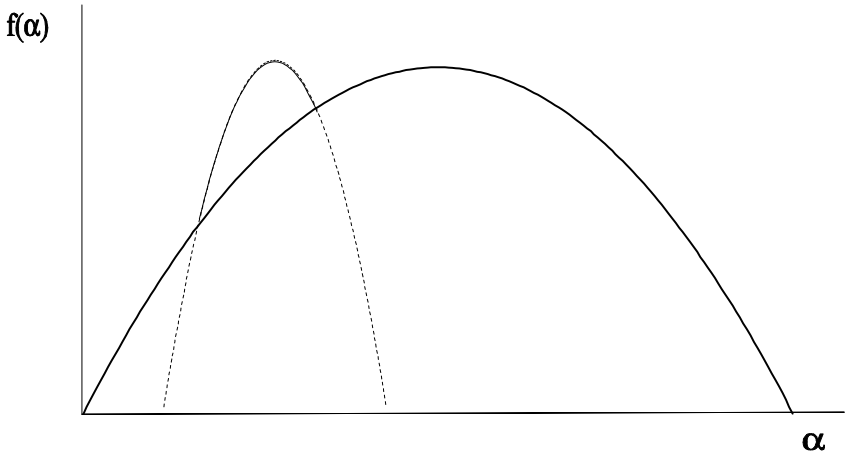

Figure 6: The spectrum of the lumping of two measures is the maximum of the individual spectra. The resulting spectrum shows clear signs of lumping and is not concave.

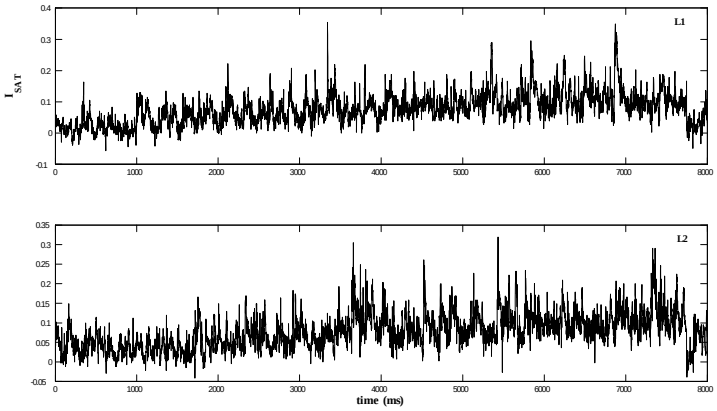

Figure 7: Saturation current fluctuations as a function of time for the low confinement regime in the Tore Supra device. Data taken during plunge 1 is labelled as L1 and plunge 2 is labelled as L2.

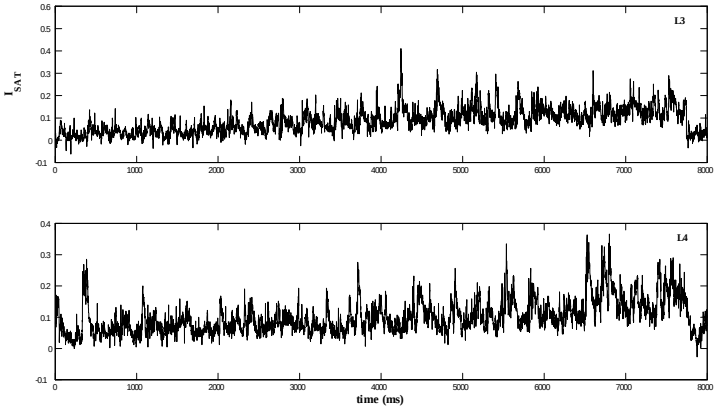

Figure 8: Saturation current fluctuations as a function of time for the low confinement regime in the Tore Supra device. Data taken during plunge 3 is labelled as L3 and plunge 4 is labelled as L4.

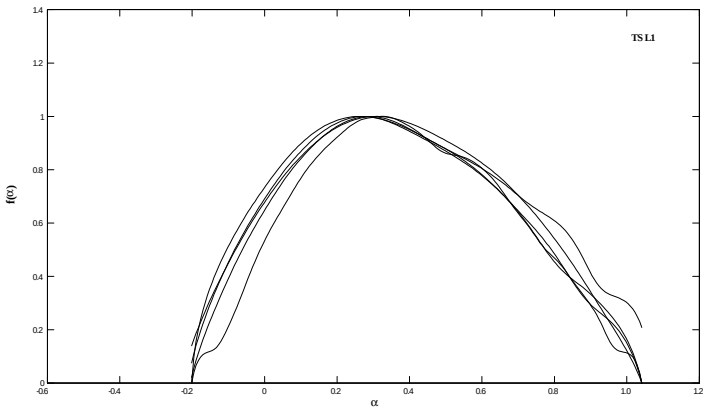

Figure 9: Large Deviation Spectrum for the L-mode signal L1 in the Tore Supra device. The spectra are almost symmetric with respect to the most probable singularity value.

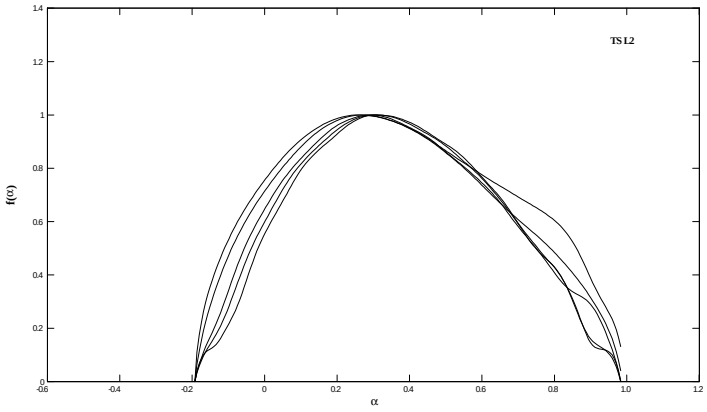

Figure 10: |Large Deviation Spectrum for the L-mode signal L2 in the Tore Supra device. Very similar to L1.

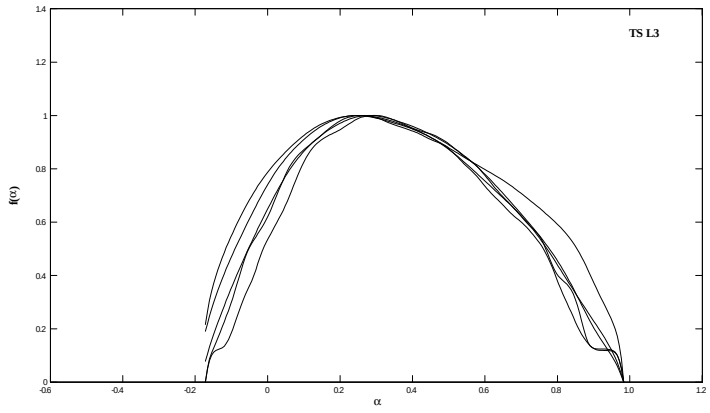

Figure 11: Large Deviation Spectrum for the L-mode signal L3 in the Tore Supra device.

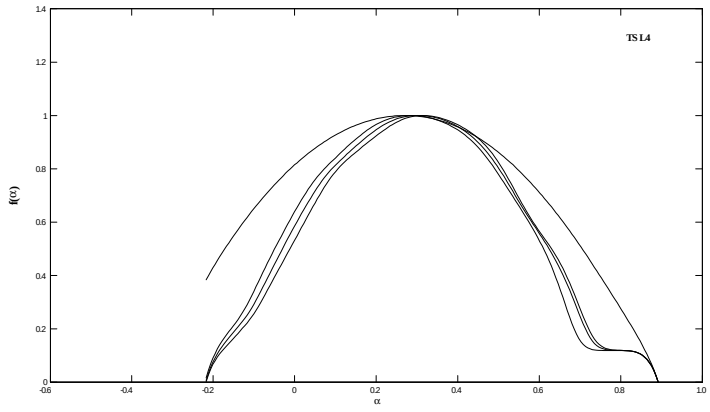

Figure 12: Large Deviation Spectrum for the L-mode signal L4 in the Tore Supra device. These spectra are the most symmetric and practiacly there is no lumping of measures.

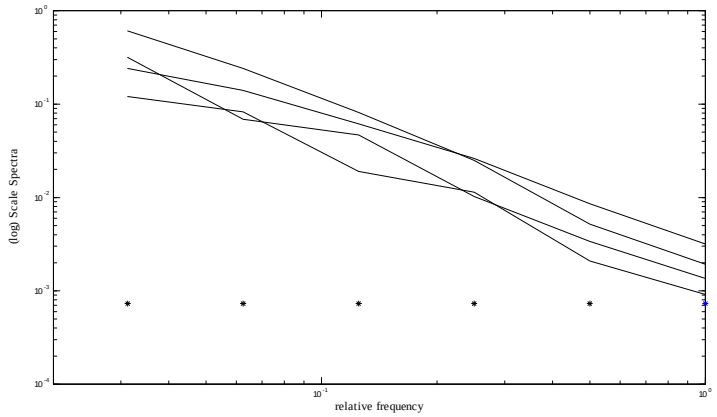

Figure 13: Scale spectra of several nonoverlapping approximately stationary segments of the L-mode signal 6861 in the MAST device. Stars represent reference Haar wavelet scales over which the power law applies i.e. the extent of inertial range.

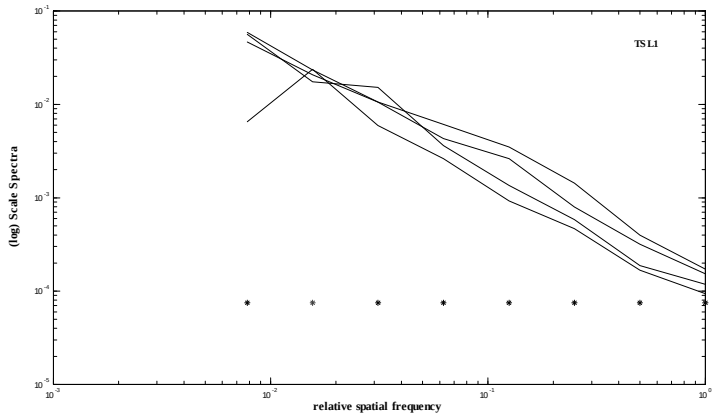

Figure 14: Scale spectra of approximately stationary nonoverlapping segments of the L-mode signal L1 in the Tore Supra device. Stars at the bottom represent reference wavelet scales over which the power law applies i.e. the extent of inertial range. Note larger extent of inertial range in the case of Tore Supra device.

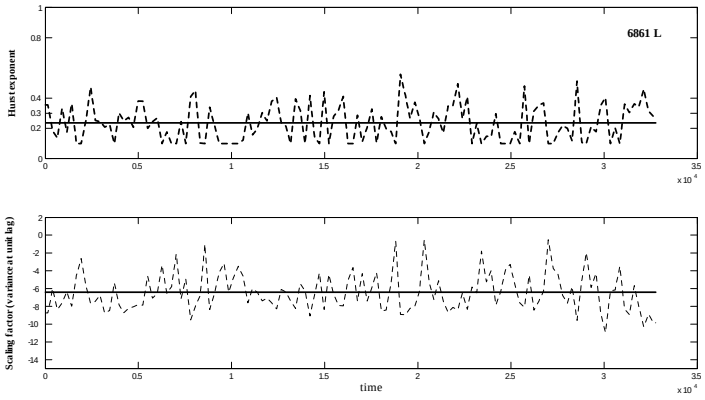

Figure 15: Parameters of the fBm model, Hurst exponent and the variance at unit lag, for the L-mode of MAST. Note random variations of each parameter reflecting mutltifractal character of the plasma density fluctuations. The smoothed vales are represented by solid lines. Note that Hurst exponent flucutates approximately around Kolmogorov's value H=1/3.

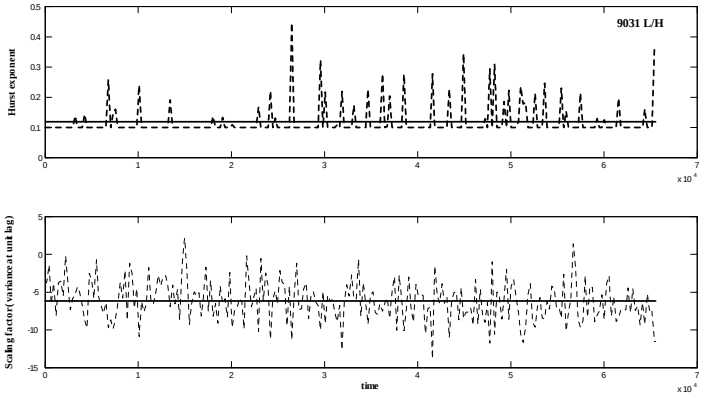

Figure 16: Parameters of the fBm model, Hurst exponent and the variance at unit lag for the dithering H-mode in MAST. Note random variations of each parameter reflecting mutltifractal character of the plasma density fluctuations. The smoothed vales are represented by solid lines. Note considerably lower value of the Hurst exponent than in the case of L-mode.

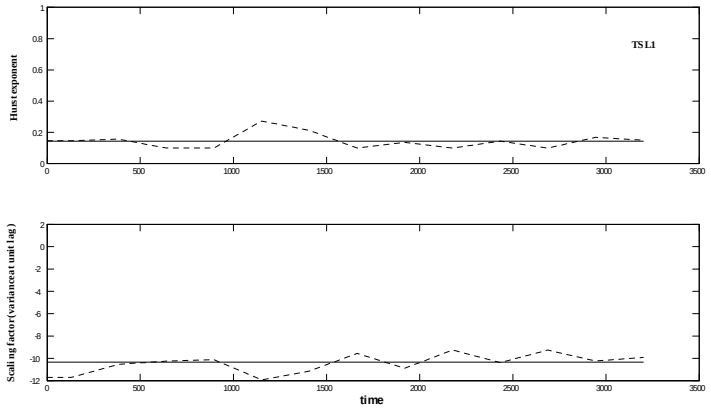

Figure 17: Parameters of the fBm model, Hurst exponent and the variance at unit lag, for the L1 fluctuations of the Tore Supra device. Note smoother, almost deterministic variations of each parameter in comaprison with random fluctuations in the MAST case.

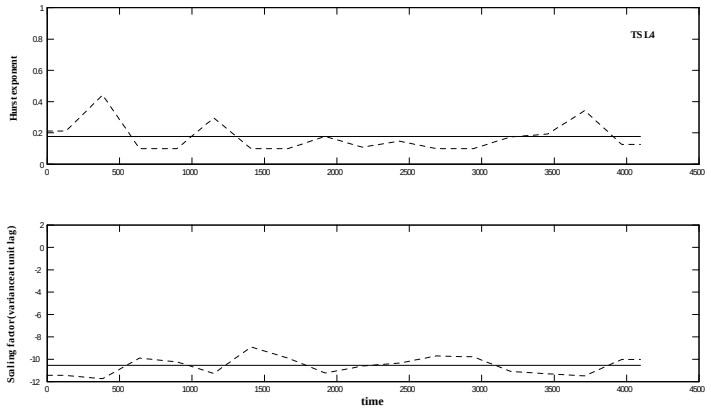

Figure 18: Parameters of the fBm model, Hurst exponent and the variance at unit lag, for the L4 signal of the Tore Supra device. Variations of these parameters is the largest among the Tore Supra data, although almost periodic variations in both parameters are readily noticeable.